Inorg. Chem. **2006**, *45*, 7621–7627

Structural and Magnetic Properties of a Complete Halide Series of Ni^{II} Complexes with a Pyridine-Containing 14-Membered Macrocycle

Abel Tamayo,[†] Lluis Escriche,[†] Carlos Lodeiro,[‡] Jordi Ribas-Ariño,[§] Joan Ribas,[∥] Berta Covelo,[‡,⊥] and Jaume Casabó*,[†]

Departament de Química, Universitat Autònoma de Barcelona, 08193 Bellaterra, Barcelona, Spain, REQUIMTE-CQFB, Departamento de Química, Universidade Nova de Lisboa, 2829-516 Monte de Caparica, Portugal, Departament de Química Física, Facultat de Química and CERQT, Parc Científic, Universitat de Barcelona, Av. Diagonal 647, 08028 Barcelona, Spain, Departament de Química Inorgànica, Universitat de Barcelona, Av. Diagonal 647, 08028 Barcelona, Spain, and Departamento de Química Inorgánica, Facultade de Química, Universidade de Vigo, 36310 Vigo, Spain

Received February 10, 2006

The complete halide series of Ni^{II} complexes containing the tetradentate macrocyclic ligand 3,11-dithia-7,17-diazabicyclo[11.3.1]heptadeca-1(17),13,15-triene (**L**), was fully characterized by X-ray diffraction. The fluoro, chloro, and bromo complexes are dinuclear species with formula $[\{Ni(\mathbf{L})\}_2(\mu\text{-}X)_2]^{2+}$ (X = halide), whereas only mononuclear species with formula $[Ni(Y)(solv)(\mathbf{L})]^{n+}$ (Y = halide or solvent molecule), were obtained with I. To date, the fluoro derivative is the first nonorganometallic coordination compound containing the $Ni(\mu\text{-}F)_2Ni$ core. The magnetic properties of these halo complexes have been studied. Intramolecular interactions were observed in the three dinuclear complexes, being antiferromagnetic in the fluoro derivative and ferromagnetic in both the chloro and bromo ones. The two iodo derivatives are paramagnetic species, as would be expected for mononuclear octahedral Ni^{II} complexes. Density functional theory calculations led us to relate the magnetic behaviors of these compounds to the values of the corresponding Ni–X–Ni' angle. The analysis of the singly occupied molecular orbitals gave a clear comprehension of the different magnetic exchange interactions found in these Ni^{II} complexes.

Introduction

In the past few decades, molecular magnetism has seen a revival because of the interest in designing new molecular materials with specific magnetic properties.[1] Indeed, the design of molecular magnetic materials, such as molecular ferromagnets and mainly single-molecule magnets (SMMs), has been one of the most interesting areas in the field of molecular magnetism. A general and basic strategy to design such materials is to organize paramagnetic centers into polynuclear aggregates by using bridging ligands, which can efficiently propagate magnetic exchange. So far, many polynuclear and extended systems of a variety of metals and ligands were designed and synthesized, and they have provided very interesting information about magneto−structural correlations in these compounds. The intimate mechanism of the magnetic exchange interactions of many polynuclear systems has been explained using density functional theory (DFT) calculations.[2]

From the classical works of Hatfield, Hodgson, and coworkers on di-μ-hydroxo complexes of Cu^{II}, it is known that the magnetic superexchange interactions between two metal ions via bridging ligands depend on the nature of both the metal ions and the connecting bridges, as well as on the geometry of the dinuclear core.[3] To fully understand the nature of the superexchange interactions, it is highly desirable to have a complete series of coordination compounds with

* To whom correspondence should be addressed. E-mail: jaume.casabo@uab.es.
[†] Universitat Autònoma de Barcelona.
[‡] Universidade Nova de Lisboa.
[§] Departament de Química Física, Facultat de Química and CERQT, Parc Científic, Universitat de Barcelona.
[∥] Departament de Química Inorgànica, Universitat de Barcelona.
[⊥] Universidade de Vigo.

(1) (a) Gatteschi, D., Kahn, O., Miller, J. S., Palacio, F., Eds. *Molecular Magnetic Materials*; NATO Advanced Study Institute Series 198; Kluwer: Dordrecht, The Netherlands, 1991. (b) Miller, J. S., Drillon, M., Eds. *Magnetism: Molecules to Materials*; Wiley-VCH: Weinheim, Germany, 2001−2005; Vols. I−V.

(2) Ruiz, E. *Struct. Bonding* **2004**, *113*, 71−102 and references cited therein.

10.1021/ic060231s CCC: $33.50
Published on Web 08/15/2006

Table 1. Crystallographic and Refinement Data for **1**, **4**, and **5**

	1	**4**	**5**
empirical formula	$C_{26}H_{40}B_2F_{10}N_4Ni_2S_4$	$C_{15}H_{25}I_2N_3NiOS_2$	$C_{14}H_{24}I_2N_2NiOS_2$
fw	865.90	640.01	612.8
cryst size (mm^3)	0.39 × 0.24 × 0.09	0.36 × 0.25 × 0.05	0.38 × 0.18 × 0.17
color/habit	cyan/plate	violet/plate	green/prism
cryst syst	monoclinic	monoclinic	monoclinic
space group	$P2_1/n$	$P2_1/c$	$P2_1/c$
a (Å)	9.386(2)	17.802(4)	16.157(3)
b (Å)	9.759(2)	8.0784(17)	8.3122(18)
c (Å)	18.572(4)	15.504(3)	16.212(3)
β (deg)	93.099(4)	108.659(4)	117.014(3)
V ($Å^3$)	1698.7(6)	1023.72(14)	1939.7(7)
Z, ρ_{calc} (g cm^{-3})	2, 1.693	4, 2.012	4, 2.099
μ (mm^{-1})	1.436	4.047	4.401
F(000)	888	1240	1184
θ range (deg)	2.20−28.31	1.21−26.40	2.52−28.30
index ranges	$-12 \le h \le 12$	$-22 \le h \le 21$	$-20 \le h \le 20$
	$-12 \le k \le 13$	$-0 \le k \le 10$	$-11 \le k \le 11$
	$-24 \le l \le 24$	$0 \le l \le 19$	$-21 \le l \le 20$
reflns collected	15 407	17 950	17 573
indep reflns (R_{int})	4092 (0.0369)	4316 (0.0294)	4672 (0.0234)
max/min transmission	0.879/0.644	0.817/0.309	0.473/0.204
GOF on F^2	1.028	1.070	1.054
final R indices	R1 = 0.0323, wR2 = 0.0672	R1 = 0.0348, wR2 = 0.0983	R1 = 0.0177, wR2 = 0.0398
final R indices (all data)	R1 = 0.0498, wR2 = 0.0745	R1 = 0.0402, wR2 = 0.1014	R1 = 0.0217, wR2 = 0.0409
largest diff peak and hole (e $Å^{-3}$)	0.641 and −0.634	1.709 and −1.915	0.439 and −0.471

the same metal complexes and different bridging ligands. Within this perspective, we report on a series of dinuclear compounds of the type $[\{Ni(\mathbf{L})\}_2(\mu\text{-}X)_2]^{2+}$ (**L** = 3,11-dithia-7,17-diazabicyclo[11.3.1]heptadeca-1(17),13,15-triene; X = F, Cl, and Br), in which the coordination geometry of the Ni^{II} ions is a distorted octahedron with two mutually cis halide bridges, which lead to the formation of three different $Ni(\mu\text{-}X)_2Ni$ cores. To the best of our knowledge, no fluoro, 45 chloro, and 4 bromo octahedral compounds of the type $[\{Ni(R)_n\}_2(\mu\text{-}X)_2]^{mq}$ (X = halide) have been, to date, completely characterized in the literature.[4]

With the final goal of finding magneto−structural correlations, we undertook experimental and theoretical magnetic studies on the $[\{Ni(\mathbf{L})\}_2(\mu\text{-}X)_2]^{2+}$ compounds. Taking into account the different experimental magnetic behavior of the fluoro complex with regard to the magnetic behavior of the analogous chloro and bromo complexes (see below), we performed theoretical calculations through DFT methodology and analysis of the singly occupied molecular orbitals (SOMOs) for the three complexes.

Experimental Section

General Remarks. Organic reagents and transition-metal salts were supplied by Aldrich and used as received. Elemental analyses were performed on a Carlo Erba EA-1108 instrument by the Chemical Analysis Service of the Universitat Autònoma de Barcelona, Bellaterra, Spain. Mass spectra were recorded using a HP298S gas chromatography/mass spectrometry (MS) system. Conductivity measurements were carried out using a Cyberscan 500 conductimeter. Absorption spectra were recorded on a Shimadzu UV-2510-PC spectrophotometer. Magnetic susceptibility measurements were made on microcrystalline samples using a Quantum Design model MPMS-XL SQUID magnetometer over a temperature range of 10−300 K with a field strength of 1 T. Macrocycle **L** and its halide Ni^{II} complexes $[\{Ni(\mathbf{L})\}_2(\mu\text{-}Cl)_2](ClO_4)_2$ (**2**) and $[\{Ni(L)\}_2(\mu\text{-}Br)_2]Br_2$ (**3**) were prepared as reported in the literature.[5]

X-ray Structure Determinations. Crystallographic data were collected at 120 K on a Bruker Smart CCD diffractometer using graphite-monochromated Mo Kα radiation (λ = 0.710 73 Å), in the RIAIDT of the University of Santiago de Compostela, Santiago de Compostela, Spain. Crystallographic data were corrected for Lorentz and polarization effects. The frames were integrated with the Bruker *SAINT*[6] software package, and the data were corrected for absorption using the program *SADABS*.[7] The structures were solved by direct methods using the program *SHELXS97*.[8] All non-H atoms were refined with anisotropic thermal parameters by full-matrix least-squares calculations on F^2 using the program *SHELXL97*.[9] H atoms were inserted at calculated positions and constrained with isotropic thermal parameters, with the exception of the H atoms of the solvent molecules and the amine groups of **4** and **5**, which were located from a Fourier difference map and refined isotropically. Special computations for the crystal structure discussions were carried out with *PLATON*.[10] Drawings were produced with *XP in SHELXTL*[11] and *SCHAKAL99*.[12] Supplementary crystallographic data have been deposited with the Cambridge Crystallographic Data Centre, CCDC No. 289337−289339 for **1**,

(3) (a) Boudreaux, E. A.; Mulay, L. N. *Theory and Applications of Molecular Paramagnetism*; John Wiley & Sons: London, 1976; Chapter 7 and references cited therein. (b) Willet, R. D., Gatteschi, D., Kahn, O., Eds. *Magneto−Structural Correlations in Exchange Coupled Systems*; NATO Advanced Study Institute Series 140; Reidel Publishing: Dordrecht, Germany, 1983.

(4) These references can be found in the Supporting Information.

(5) Tamayo, A.; Casabó, J.; Escriche, L.; Lodeiro, C.; Covelo, B.; Brondino, C. D.; Kivekäs, R.; Sillampää, R. *Inorg. Chem.* **2006**, *45*, 1140−1149.

(6) *SMART (control) and SAINT (integration) software*; Bruker Analytical X-ray Systems: Madison, WI, 1994.

(7) Sheldrick, G. M. *SADABS, A Program for Absorption Corrections*; University of Göttingen: Göttingen, Germany, 1996.

(8) Sheldrick, G. M. *SHELXS97, A Program for the Solution of Crystal Structures from X-ray Data*; University of Göttingen: Göttingen, Germany, 1997.

(9) Sheldrick, G. M. *SHELXL97, A Program for the Refinement of Crystal Structures from X-ray Data*; University of Göttingen: Göttingen, Germany, 1997.

(10) Spek, A. L. *PLATON, A Multipurpose Crystallographic Tool*; Utrecht University: Utrecht, The Netherlands, 2004.

(11) *XP in SHELTXL, Interactive Molecular Graphics*, version 5.1; Bruker Analytical X-ray Systems: Madison, WI, 1998.

5, and **4**, respectively. The crystallographic parameters are summarized in Table 1.

Theoretical Calculations. DFT calculations[13] were carried out using *Gaussian 03*,[14] which was implemented with the B3LYP gradient-corrected density functional[15] and an Ahlrich pVDZ basis set.[16] The broken-symmetry[17] procedure was used to evaluate the singlet state energy. The values of the J parameters (for the $H = -JS_1S_2$ Hamiltonian) were obtained as $J = [E(\mathrm{T}) - E(\mathrm{S,BS})]/2$, where E(T) is the energy for the triplet state and E(S,BS) is the energy for the broken-symmetry singlet. Because we were only interested in qualitative trends, the macrocycle ligand was replaced by ammonia and dimethyl sulfide ligands in order to lower the computational effort.

[{Ni(L)}$_2$(μ-F)$_2$](BF$_4$)$_2$ (1). This complex was prepared as reported in the literature.[5] Cyan crystals suitable for X-ray structure determination were obtained by slow evaporation of an acetonitrile solution of **1**.

[Ni(CH$_3$CN)(H$_2$O)(L)]I$_2$ (4). This complex was prepared according to a previously described procedure.[5] Violet crystals suitable for X-ray structure determination were obtained by slow diffusion of diethyl ether into an acetonitrile solution of **4**. Conductivity (CH$_3$CN, 1×10^{-3} M): 131 μS cm^{-1}.

[NiI(CH$_3$OH)(L)]I (5). This complex was isolated from a methanol solution of **4** as green crystals suitable for X-ray structure determination. Conductivity (CH$_3$OH, 1×10^{-3} M): 101 μS cm^{-1}. ESIMS (m/z): 453.0 [NiI(**L**)]$^+$. UV−vis [CH$_3$OH, λ, nm (ϵ, M^{-1} cm^{-1})]: 663 (83), 860 (36).

Results and Discussion

Synthesis. We have previously reported the synthesis of the pyridine-containing 14-membered macrocycle **L** and its fluoro (**1**), chloro (**2**), bromo (**3**), and iodo (**4**) Ni^{II} complexes, as well as the X-ray crystallographic studies of **2** and **3**.[5] These crystal structures showed that the chloro and bromo complexes are dinuclear species with [{Ni(**L**)}$_2$(μ-X)$_2$]$^{2+}$ cations, in which two Ni**L** moieties are linked by two halide bridges. The analytical data of **1** suggested that the fluoro complex is analogous to the chloro and bromo complexes. On the other hand, the analytical data of the iodo complex **4** suggested that it is a mononuclear compound.

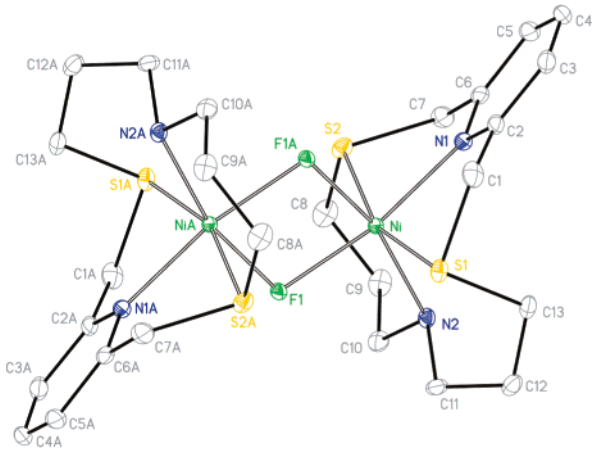

Figure 1. Displacement ellipsoid representation (at the 30% probability level) of the [{Ni(**L**)}$_2$(μ-F)$_2$]$^{2+}$ ion, with the atom-numbering scheme adopted. Noncoordinated counterions and H atoms were omitted for clarity.

The three crystal structures reported in the present paper agree well with those data because the structure of the fluoro complex corresponds to a dinuclear compound with two fluoride bridges between two Ni**L** units, whereas the two structures of the iodo complex corresponds to mononuclear species. The iodo complex **4** was previously reported as [NiI(CH$_3$CN)(**L**)]I because this is the formula that agrees well with its elemental analysis, conductivity measurements, mass spectroscopy, and electronic spectrum.[5] In the present work, this complex has been reformulated as [Ni(CH$_3$CN)(H$_2$O)(**L**)](I)$_2$ because, as reflected in its crystal structure, no iodide ion is coordinated to the metal center in the solid state. The change of the coordination sphere of the metal center from solution to solid state is evidenced by comparing the color of an acetonitrile solution of **4** (yellow-green) with the color of the crystals that grow into it (purple). This color change was not observed when methanol was used as the solvent instead of acetonitrile because green crystals were obtained from a green solution of **4** in methanol. The X-ray studies of these crystals indicate that one iodide is coordinated to each Ni^{II} ion, and the conductivity measurements indicate that this halide ion is also coordinated to the metal center in a methanol solution. These data together with the elemental analysis of these crystals suggest that this complex should be formulated as [NiI(CH$_3$OH)(**L**)]I (**5**).

X-ray Structures. Figures 1 and 2A,B show drawings of the complex cations of **1**, **4**, and **5**, respectively. Selected bond lengths and angles are summarized in Table 2.

The crystal structure of **1** is similar to those recently reported for the chloro and bromo complexes **2** and **3**[5] and consists of [{Ni(**L**)}$_2$(μ-F)$_2$]$^{2+}$ cations and tetrafluoroborate counterions. The halves of the dinuclear cation are related by the crystallographically imposed center of symmetry. The coordination geometry around the Ni^{II} ions is a distorted octahedron with two mutually cis halide bridges and the two N atoms and two S atoms of one **L** molecule, which adopts a folded conformation. The Ni−F bond lengths [2.0041(13) and 2.0169(13) Å] and the F−Ni−F^i and Ni−F−Ni^i angles [79.73(5)° and 100.27(5)°, respectively] define a NiF$_2$Ni plane with symmetry code i: $1 - x$, $1 - y$, $1 - z$. The Ni−N$_{py}$ [2.0870(19) Å], Ni−N$_{aliphatic}$ [2.1154(19) Å], and Ni−S

(12) Keller, E. *SCHAKAL99. A Computer Program for the Graphic Representation of Molecular and Crystallographic Models*; University of Freiburg: Freiburg, Germany, 1999.
(13) Parr, R. G.; Yang, W. *Density Functional Theory of Atoms and Molecules*; Oxford University Press: New York, 1989.
(14) Frisch, M. J.; Trucks, G. W.; Schlegel, H. B.; Scuseria, G. E.; Robb, M. A.; Cheeseman, J. R.; Montgomery, J. A.; Vreven, T., Jr.; Kudin, K. N.; Burant, J. C.; Millam, J. M.; Iyengar, S. S.; Tomasi, J.; Barone, V.; Mennucci, B.; Cossi, M.; Scalmani, G.; Rega, N.; Petersson, G. A.; Nakatsuji, H.; Hada, M.; Ehara, M.; Toyota, K.; Fukuda, R.; Hasegawa, J.; Ishida, M.; Nakajima, T.; Honda, Y.; Kitao, O.; Nakai, H.; Klene, M.; Li, X.; Knox, J. E.; Hratchian, H. P.; Cross, J. B.; Adamo, C.; Jaramillo, J.; Gomperts, R.; Stratmann, R. E.; Yazyev, O.; Austin, A. J.; Cammi, R.; Pomelli, C.; Ochterski, J. W.; Ayala, P. Y.; Morokuma, K.; Voth, G. A.; Salvador, P.; Dannenberg, J. J.; Zakrzewski, V. G.; Dapprich, S.; Daniels, A. D.; Strain, M. C.; Farkas, O.; Malick, D. K.; Rabuck, A. D.; Raghavachari, K.; Foresman, J. B.; Ortiz, J. V.; Cui, Q.; Baboul, A. G.; Clifford, S.; Cioslowski, J.; Stefanov, B. B.; Liu, G.; Liashenko, A.; Piskorz, P.; Komaromi, I.; Martin, R. L.; Fox, D. J.; Keith, T.; Al-Laham, M. A.; Peng, C. Y.; Nanayakkara, A.; Challacombe, M.; Gill, P. M. W.; Johnson, B.; Chen, W.; Wong, M. W.; Gonzalez, C.; Pople, J. A. *Gaussian 03*, revision C.02; Gaussian, Inc.: Wallingford, CT, 2004.
(15) Becke, A. D. *J. Chem. Phys.* **1993**, *98*, 5648−5652.
(16) Schaefer, A.; Horn, H.; Ahlrichs, R. *J. Chem. Phys.* **1992**, *97*, 2571−2577.
(17) Noodlemann, L. *J. Chem. Phys.* **1981**, *74*, 5737−5743.

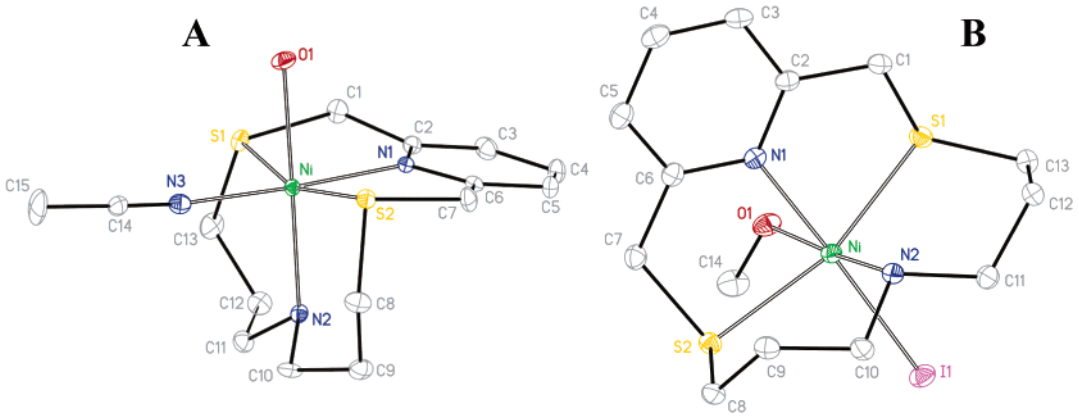

Figure 2. Structure of complexes $[Ni(CH_3CN)(H_2O)(\mathbf{L})]^{2+}$ (A) and $[NiI(CH_3OH)(\mathbf{L})]^{+}$ (B), with the atom-numbering scheme adopted. Ellipsoids are shown at the 40% probability level. Noncoordinated counterions and H atoms were omitted for clarity.

Table 2. Selected Bond Lengths (Å) and Angles (deg) for **1**, **4**, and **5**[a]

	1	4	5
Ni−N1	2.0870(19)	2.066(4)	2.0719(17)
Ni−N2	2.1154(19)	2.121(4)	2.1250(18)
Ni−N3		2.041(5)	
Ni−O1		2.160(4)	2.2022(16)
Ni−S1	2.4568(8)	2.4055(14)	2.3592(7)
Ni−S2	2.4016(8)	2.3794(14)	2.3854(6)
Ni−X1	2.0041(13)		2.7145(5)
Ni−X1^{i}	2.0169(13)		
S1−Ni−S2	161.67(2)	163.65(5)	163.38(2)
N1−Ni−N2	104.86(8)	92.19(17)	92.16(7)
N1−Ni−N3	N(1)−Ni−N(3)	177.02(18)	
N2−Ni−N3	N(2)−Ni−N(3)	90.76(18)	
N1−Ni−O1		89.26(16)	84.92(6)
N2−Ni−O1	N(2)−Ni−O(1)	177.79(16)	176.59(7)
N3−Ni−O1	N(3)−Ni−O(1)	87.78(17)	
S1−Ni−N1	80.84(5)	84.94(12)	82.30(5)
S1−Ni−N2	91.55(5)	97.58(12)	91.94(5)
S1−Ni−N3		95.08(13)	
S2−Ni−N1	80.97(6)	84.14(13)	85.32(5)
S2−Ni−N2	95.28(5)	94.97(12)	99.58(5)
S2−Ni−N3		95.20(13)	
S1−Ni−O1		84.21(11)	85.94(4)
S2−Ni−O1		83.51(11)	81.95(4)
X1−Ni−O1		84.21(11)	88.72(4)
Ni−X1−Ni^{i}	100.27(5)		
X1−Ni−X1^{i}	79.73(5)		
X1−Ni−S1	100.17(4)		97.66(2)
X1^{i}−Ni−S1	87.18(4)		
X1−Ni−S2	97.24(4)		93.42(2)
X1^{i}−Ni−S2	90.35(4)		
X1−Ni−N1	168.89(6)		173.62(5)
X1^{i}−Ni−N1	89.29(6)		
X1−Ni−N2	86.21(7)		94.22(5)
X1^{i}−Ni−N2	165.42(6)		

[a] i: $1-x, 1-y, 1-z$.

[2.4568(8) and 2.4016(8) Å] distances are a little longer than those found in the analogous chloro and bromo dinuclear complexes **2** and **3**. The Ni−S bond lengths lie within the range observed for similar macrocyclic-containing dinuclear complexes.[18] The structure of **1** is the first with organic ligands in which two octahedral Ni^{II} ions are bridged by two fluoride ions because, although Radonovich and co-workers reported the structure of an organic compound with a Ni-(μ-F)$_2$Ni core, it is, in fact, an organometallic compound with square-planar Ni^{II} ions.[19] In addition, two structures with only one fluoride ion bridging two octahedral Ni^{II} ions have been reported (Ni−F bond lengths between 1.967 and 1.984 Å).[18b,20] For **1**, the Ni···Ni and F···F distances (3.0863 and 2.5775 Å, respectively) are slightly larger than those found in the above-mentioned organometallic compound.

Table 3. Comparison of Selected Bond Parameters[a,b]

	Ni−X	Ni−X^{i}	Ni···Ni^{i}	X···X^{i}	X−Ni−X^{i}	Ni−X−Ni^{i}
1	2.0041(13)	2.0169(13)	3.086	2.578	79.73(5)	100.27(5)
2	2.3811(6)	2.5350(7)	3.583	3.370	86.48(2)	93.52(2)
3	2.5228(6)	2.7686(7)	3.840	3.649	87.06(2)	92.94(2)
5	2.7145(5)					

[a] X = F for **1**, Cl for **2**, Br for **3**, and I for **5**. [b] i = $1-x, 1-y, 1-z$ for **1**; $-x, -y, 1-z$ for **2**; and $1-x, 1-y, -z$ for **3**.

The crystal structures of **4** and **5** consist of $[Ni(CH_3CN)(H_2O)(\mathbf{L})]^{2+}$ and $[NiI(CH_3OH)(\mathbf{L})]^{+}$ cations, respectively, and iodide counteranions. Both cations have one Ni^{II} ion coordinated to one **L** molecule by two N atoms and two S atoms. This ligand molecule adopts a folded conformation, which leaves the other two coordination sites in a relative cis orientation. These two available sites are occupied by water and acetonitrile molecules in **4** and iodide and methanol molecules in **5**. The Ni−N_{py} [2.066(4) Å for **4** and 2.0719(17) Å for **5**], Ni−$N_{aliphatic}$ [2.121(4) Å for **4** and 2.1250(18) Å for **5**], and Ni−S [2.4055(14) and 2.3794(14) Å for **4** and 2.3592(7) and 2.3854(6) Å for **5**] distances are similar to those found in analogous Ni^{II} complexes.[5,21]

Selected bond lengths and angles for **1**−**3** and **5** are listed in Table 3. As shown in this table, the bigger the halide ion, the larger the difference between its Ni−X bond lengths and, therefore, the more asymmetric the Ni(μ-X)$_2$Ni core. In fact, whereas this moiety is almost symmetric in the fluoro complex **1**, it is significantly asymmetric in the bromo complex

(18) Blake, A. J.; Halcrow, M. A.; Schröder, M. *J. Chem. Soc., Dalton Trans.* **1994**, *9*, 1463−1470. (b) Blake, A. J.; Devillanova, F. A.; Garau, A.; Harrison, A.; Isaia, F.; Lippolis, V.; Tiwary, S. K.; Schröder, M.; Verani, G.; Whittaker, G. *J. Chem. Soc., Dalton Trans.* **2002**, *23*, 4389−4394.
(19) Brezinski, M. M.; Schneider, J.; Radonovich, L. J.; Klabunde, K. J. *Inorg. Chem.* **1989**, *28*, 2414−2419.
(20) Emsley, J.; Arif, M.; Bates, P. A.; Hursthouse, M. B. *J. Chem. Soc., Dalton Trans.* **1989**, *7*, 1273−1276.
(21) (a) Drew, M. G. B.; Hollis, S. *Acta Crystallogr.* **1980**, *B36*, 2629−2632. (b) Constable, E. C.; Lewis, J.; Marquez, V. E.; Raithby, P. R. *J. Chem. Soc., Dalton Trans.* **1986**, *8*, 1747−1749. (c) Adhikary, B.; Liu, S.; Lucas, C. B. *Inorg. Chem.* **1993**, *32*, 5957−5962. (d) Vetrichelvan, M.; Lai, Y.-H.; Mok, K. F. *Dalton Trans.* **2003**, *3*, 295−303.

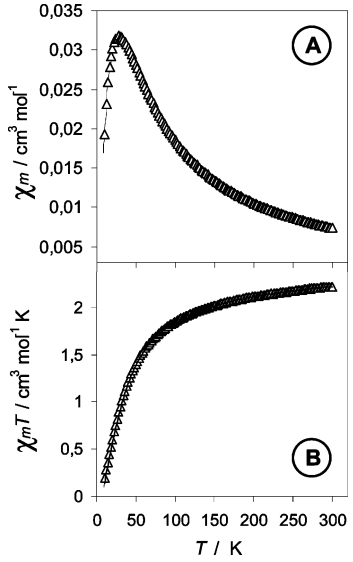

Figure 3. Plots of experimental χ_m (A) and χ_mT (B) vs T for complex **1**. The solid lines are the best fits obtained from least-squares regression.

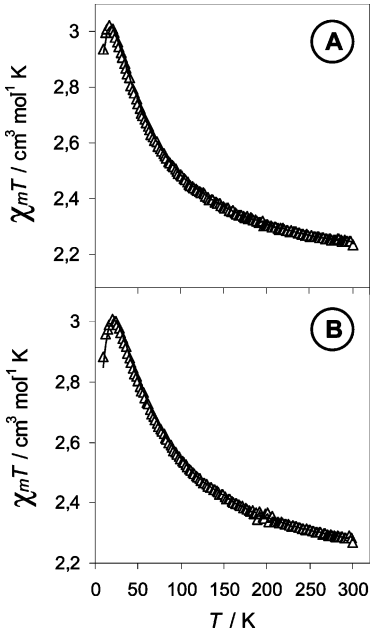

Figure 4. Plots of experimental χ_mT vs T for complexes **2** (A) and **3** (B). The solid lines are the best fits obtained from least-squares regression.

3. The asymmetry may be due to steric impediments between the two halide bridges of a dinuclear complex, which in the limit would not allow the formation of the analogous Ni^{II} complex with two iodide bridges.

Several intermolecular interactions were found in the crystal structures of **1**−**5**. The existence of $\pi\cdots\pi$ interactions[22] between pyridine rings of neighboring dinuclear moieties in **1** leads to the formation of one-dimensional arrangements along the crystallographic *b* axis (Figure S1 in the Supporting Information).[23] In this chain, the shortest Ni···Ni distance is 8.602 Å. On the other hand, in the structures of **2**−**5**, H bonds[24] between the cationic complexes and their counteranions are the intermolecular interactions responsible for the formation of one-dimensional arrangements (Figures S2−S5 in the Supporting Information). In the structures of complexes **2** and **3**, these H bonds are formed between N−H groups of **L** molecules and the respective counteranions, as well as between C−H groups of **L** molecules and these same counteranions.[25] Within these chains, the shortest Ni···Ni distances are 9.659 and 9.049 Å for **2** and **3**, respectively. In the structures of complexes **4** and **5**, there are also two kinds of H bonds that lead to the formation of one-dimensional arrangements, in which N−H groups of **L** molecules and O−H groups of coordinated solvent molecules act as donors and iodide counteranions act as acceptors.[26] In these chains, the shortest Ni···Ni distances are 7.771 and 9.061 Å for **4** and **5**, respectively.

Magnetic Properties. Figure 3 shows the temperature dependence of χ_m and χ_mT for complex **1**.[27] At 300 K, the χ_m value is 0.0075 cm^3 mol^{-1}. An increase in χ_m is observed upon a decrease in the temperature, leading to a maximum of 0.032 cm^3 mol^{-1} at 25 K. Below this temperature, χ_m rapidly decreases to 0.018 cm^3 mol^{-1} at 10 K (Figure 3A). This pattern suggests the presence of a noticeable intramolecular antiferromagnetic interaction. Figure 3B shows that, at 300 K, the χ_mT product is 2.25 cm^3 mol^{-1} K, which is approaching the value for two magnetically isolated spin triplets ($g > 2.00$). As the temperature is decreased, there is a steady decrease in χ_mT down to the final value of 0.2 cm^3 mol^{-1} K at 10 K. This behavior is again consistent with intramolecular antiferromagnetic coupling between the two Ni^{II} ions.

Table 4. Best Fit of the Magnetic Parameters

compound	J (cm^{-1})	g	J' (cm^{-1})	D (cm^{-1})
1 (fit χ_m)	−19.60	2.15		
1 (fit χ_mT)	−20.67	2.17		
2 (fit χ_mT)	21.07	2.05	−0.28	
2 (fit χ_mT)	19.90	2.06		12.0
3 (fit χ_mT)	23.82	2.05	−0.23	
3 (fit χ_mT)	22.73	2.05		11.6

To confirm this qualitative interpretation, the experimental data in parts A and B of Figure 3 were fit to the known formula for dinuclear Ni^{II} compounds, which was derived from the spin Hamiltonian $H = -JS_1S_2$. The best fits are listed in Table 4. We can state that the J value is between −19.6 and −20.7 cm^{-1} and the g value is between 2.15 and 2.17, with R values on the order of 10^{-6}, indicating good fits.[28]

The temperature dependence of the χ_mT product for complex **2** is shown in Figure 4A. At 300 K, the χ_mT value is 2.28 cm^3 mol^{-1} K, as would be expected for two magnetically isolated spin triplets. Starting from room temper-

(22) Janiak, C. *J. Chem. Soc., Dalton Trans.* **2000**, *21*, 3885−3896.
(23) Cg(1)···dCg(1)^i distance: 3.59 Å. Symmetry code i: $1-x, -y, 1-z$. Dihedral angle α: 0.02°.
(24) (a) Beatty, A. M. *CrystEngComm* **2001**, *51*, 1−13. (b) Beatty, A. M. *Coord. Chem. Rev.* **2003**, *246*, 131−143. (c) Desiraju, G. R. *Chem. Commun.* **2005**, *24*, 2995−3001.
(25) H bond distances: N···O 3.304 Å and C···O 3.319−3.488 Å for **2** and N···Br 3.423 Å and C···Br 3.668 Å for **3**.
(26) H bond distances: N···I 3.644 Å for **4** and 3.725 Å for **5** and O···I 3.414 Å for **4** and 3.528 Å for **5**.
(27) χ_m is the molar magnetic susceptibility for two Ni^{2+} ions.
(28) R is the agreement factor defined as $\sum_i[(\chi_mT)_{obs} - (\chi_mT)_{calc}]^2/\sum_i[(\chi_mT)_{obs}]^2$.

ature, the $\chi_m T$ values increase monotonically to 3.0 $cm^3\ mol^{-1}$ K at 20 K and then slightly decrease to 2.95 $cm^3\ mol^{-1}$ K at 10 K. The increase from room temperature to 20 K is a clear signature of intramolecular ferromagnetic coupling, whereas the final decrease indicates the presence of either antiferromagnetic intermolecular interactions or zero-field-splitting contributions (D parameter). Figure 4B shows the temperature dependence of the $\chi_m T$ product for complex **3**. The $\chi_m T$ value at 300 K (2.27 $cm^3\ mol^{-1}$ K), its increase until 20 K (3.05 $cm^3\ mol^{-1}$ K), and its decrease at lower temperatures (2.9 $cm^3\ mol^{-1}$ K at 10 K) are analogous to those observed for complex **2**, which suggests similar magnetic properties for both complexes.

From the Hamiltonian $H = -JS_1S_2$, the fit of the susceptibility data for **2** and **3** was carried out by applying two different approaches: considering either the J' parameter (by means of molecular-field approximation) or a full-diagonalization program in which the D parameter is taken into consideration.[29] The best-fit parameters obtained by applying these two approaches are listed in Table 4. In all cases, the positive sign of the J values (between 19.9 and 23.8 cm^{-1}) indicates that **2** and **3** are ferromagnetic species, with g values around 2.05, J' values between -0.23 and -0.28 cm^{-1}, and the D parameter slightly larger than 10 cm^{-1}.[30] R values were in all cases on the order of 10^{-6}. As occurs in many of these calculations, the D parameter is overestimated when the J' value is not taken into account. For a single Ni^{II} ion, the D parameter is around 10 cm^{-1}, whereas the standard value for isolated Ni^{II} complexes is close to 6 cm^{-1}.[31] Therefore, the higher-than-expected values of the D parameter for **2** and **3** indicate the presence of antiferromagnetic interactions, which, although small, should be taken into account. It must be emphasized that there is practically no dependence of D on the J value (see Figure S6 in the Supporting Information).

Both iodo derivatives (compounds **4** and **5**) are paramagnetic species, as would be expected for mononuclear octahedral Ni^{II} complexes.

Theoretical Studies. DFT calculations were performed in order to understand why the magnetic behavior of complex **1** is different from the magnetic behavior of complexes **2** and **3**. One of the main structural differences between the fluoro compound **1** and both the chloro and bromo compounds **2** and **3**, respectively, is the value of the Ni−X−Ni^i bond angle (X = halide). In the case of **1**, this value is 100.3°, whereas in the cases of **2** and **3**, the angles are 93.5° and 92.9°, respectively. DFT calculations were carried out in order to know if the Ni−X−Ni^i angle is the structural factor that determines the sign and magnitude of the exchange coupling constant J between the Ni^{II} ions. The three dinuclear complexes exhibit the same qualitative behavior when the calculated J values are plotted versus the Ni−X−Ni^i angle (Figure 5). As the angle increases, the J values become less ferromagnetic and they even change their sign, thus becoming

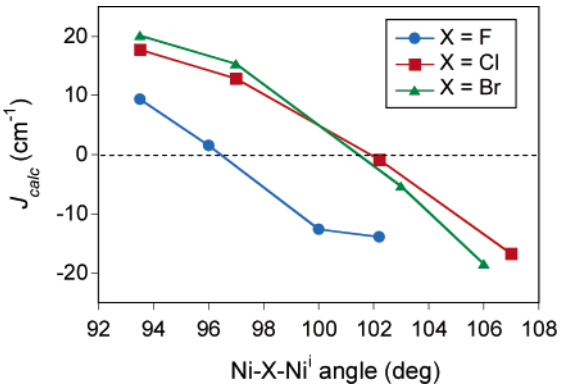

Figure 5. Plot of calculated J values vs Ni−X−Ni^i angles.

antiferromagnetic. The experimental angle for the fluoro compound is expected to yield an antiferromagnetic interaction, while the experimental angles for the chloro and bromo compounds are expected to be associated with ferromagnetic interactions. These theoretical results are in excellent agreement with the experimental observations, which suggests the existence of a significant relationship between the value of the Ni−X−Ni^i bond angle and the sign and magnitude of the J values.

This relationship between the angles and the J values can be qualitatively understood by analyzing the molecular orbitals according to the Hoffmann theory.[32] The SOMOs for the experimental geometries of **1**−**3** and their corresponding energies are given in Figure S7 in the Supporting Information. According to our DFT calculations, the fluoro complex has a significant difference between the energies of the $d_{x^2-y^2}$-like orbitals (Figure S7A in the Supporting Information). On the contrary, for the chloro and bromo complexes, this energy difference is practically negligible (parts B and C in Figure S7 in the Supporting Information, respectively). Because the energy difference between the d_{z^2}-like orbitals is similar and small in the three cases, the J_{AF} component of the fluoro complex is greater than those of the chloro and bromo complexes. In what concerns the J_F component, looking at Figure S7 in the Supporting Information, it can be seen that there is a noticeable spin density on the bridging atoms. This feature can give rise to a noticeable J_F component, thus yielding ferromagnetic coupling. In the case of the fluoro complex, the J_{AF} component created by the energy difference between the $d_{x^2-y^2}$-like orbitals is the dominant pathway and completely masks the J_F component.

Conclusions

A complete series of the halide Ni^{II} complexes containing ligand **L** was studied crystallographically. The fluoro, chloro, and bromo derivatives are dinuclear species in which two halide ions bridge two Ni**L** moieties. The larger the halide ion, the more asymmetric the Ni(μ-X)$_2$Ni core, which in the limit leads to the formation of mononuclear species with iodide ions.

$\pi\cdots\pi$ interactions between pyridine rings of **L** molecules for **1** and H bonds between N−H groups of **L** and the

(29) This program was made and gently supplied to us by Prof. V. Tangoulis from the University of Patras, Patras, Greece.
(30) It is important to mention that J' and D are always strongly correlated.
(31) Boca, R. *Coord. Chem. Rev.* **2004**, *248*, 757−815.
(32) Hay, P. J.; Thibeault, J. C.; Hoffmann, R. *J. Am. Chem. Soc.* **1975**, *97*, 4884−4899.

respective counteranions for **2**−**5** lead to the formation of self-assembly structures.

The analysis of the DFT calculations gives a clear and pedagogical comprehension of the antiferromagnetic coupling in the fluoro compound **1** and the ferromagnetic coupling in the chloro and bromo derivatives **2** and **3**, respectively. In these last two compounds, the orthogonality of the corresponding orbitals indicates the lack of antiferromagnetic coupling but not necessarily the existence of a noticeable J_F component. This J_F component exists because the spin density in the bridging zone is not zero, mainly in the corresponding d_{z^2}-like orbitals.

Acknowledgment. This work was supported by the Spanish Government (CYCIT) under Project CTQ2004-04134 and by the Catalan Government (DURSI) via Grant FI2002-00320 (A.T.). Financial support by the Fundação para a Ciência e Tecnologia (Portugal) and FEDER (Projects POCI/QUI/55519/2004 and POCTI/QUI/47357/2002) is also acknowledged.

Supporting Information Available: X-ray crystallographic data in CIF format for complexes **1**, **4**, and **5**, CSD search for structures of Ni^{II} complexes containing $Ni(\mu\text{-}X)_2Ni$ cores, figures of the crystallographic interactions between neighboring units in complexes **1**−**5**, dependence of *D* on the *J* value, and calculated SOMOs for complexes **1**−**3**. This material is available free of charge via the Internet at http://pubs.acs.org.

IC060231S